引用格式：YU Yue, SI Haoxuan, YANG Zuhua, et al. Design and Experimental Study of a Desktop Monochromatic X-ray Source Based on Spherical Bent-crystal Focusing Structure[J]. Acta Photonica Sinica, 2023, 52(7):0734001
余越,司昊轩,杨祖华,等.基于球面弯晶聚焦结构的桌面型单能X射线源设计及实验[J].光子学报,2023,52(7):0734001

基于球面弯晶聚焦结构的桌面型单能X射线源设计及实验

余越[1,2],司昊轩[1,2],杨祖华[3],伊圣振[1,2],王占山[1,2]
(1 同济大学 物理科学与工程学院 精密光学工程技术研究所,上海 200092)
(2 同济大学 先进微结构材料教育部重点实验室,上海 200092)
(3 中国工程物理研究院 激光聚变研究中心,绵阳 621900)

摘　要:提出了一种采用球面弯晶聚焦结构获得高亮度桌面型单能X射线的方法。在子午方向利用晶体色散实现单能、在弧矢方向通过球面镜聚焦提高光强。理论建模和光学仿真评估了该结构的色散和聚焦性能,验证了球面弯晶聚焦结构相对于柱面弯晶在聚焦特性上的显著优势。针对Al靶$K\alpha_1$线单能需求,设计和装调了基于低功率Al靶X射线管的单能装置,并实验验证了其性能。结果显示,当X射线管工作在7 W功率条件下,CCD曝光10 min,Al靶$K\alpha_1$线全视场光谱的探测器计数大于2×10^5,能谱展宽约为0.592 eV;引入200 μm限束光阑,能谱展宽进一步减小至0.493 eV,探测器计数约为2×10^4。研究结果证实了该装置可以有效获得高亮度Al靶$K\alpha_1$谱线,也为精确测量光学器件和系统的光谱特性提供了一种新的获得高亮度单能X射线的技术途径。

关键词:球面弯晶聚焦;高亮度;高单能性;桌面型;X射线源
中图分类号:O434　　**文献标识码**:A　　**doi**:10.3788/gzxb20235207.0734001

0 引言

X射线光学器件和系统已广泛应用在了等离子体诊断、X射线谱学分析、天文观测和材料分析等领域[1-5],通常针对特定的工作能点设计,因而其能谱响应特性需要精确测量。高亮度的单能X射线源是实现精确测量的基础。同步辐射光源具有光谱宽且连续、偏振度高、亮度强、方向性好等特点,是标定X射线器件及系统的理想光源[6-8],但其机时有限,难以满足测试的及时性。高准直度的光束线也难以模拟某些应用的实际光源环境,如激光等离子体诊断实验中的发散光源。商用的X射线检测设备,如X射线荧光光谱仪、X射线衍射仪等[9-10],其光源部分高度封装且样品放置空间有限,只能在少数能点测试较小型器件的光谱响应。

基于实验室条件搭建的桌面型单能X射线源,利用X射线管结合滤波或色散器件的方式实现单能X射线。其中X射线管多为微焦点源,单色器件通常选择多层膜反射镜、光栅或晶体。多层膜反射镜由高、低折射率材料交替镀制,通过各界面反射波的相长干涉提高反射率[11-13]。其光通量高、工作能段较宽,但能谱分辨率在X射线波段只有10^2至10^3。以光栅作为分光器件可以获得更高的能谱分辨率,在X射线波段达到10^3至10^4[14,15]。但X射线光栅刻痕周期非常小,进一步提高分辨率需要更小的刻痕间隔,这对制作工艺要求极高。

晶体在X射线波段具有天然的色散能力[16],可将能谱分辨率提升至10^5。常用的晶体面形包括平面、柱面、球面以及更复杂的非球面等。其中,平面晶体仅在波长方向色散,没有聚焦功能,需要在光路中引入额

基金项目:国家重点研发计划(Nos. 2022YFA1603500, 2019YFE03080200),国家自然科学基金(Nos. 11875202, 12105268)
第一作者:余越,1730999@tongji.edu.cn
通讯作者:王占山,wangzs@tongji.edu.cn; 伊圣振,023123@tongji.edu.cn
收稿日期:2023-03-06;**录用日期**:2023-04-04

外的透镜组实现准直或聚焦。柱面晶体可以在波长方向上同时实现色散和聚焦，但在空间方向上不具有聚焦功能，无法有效提高系统光通量[17]。超环面、抛物面、双曲面等复杂的非球面弯晶可以在子午和弧矢方向同时聚焦，大幅减小像差并提高能谱分辨率[18-19]。但是非球面弯晶的制备难度较高、应用限制较多，且如果其工作角度偏离衍射角，像差会骤增。球面弯晶在波长和空间方向上都可以聚焦，且制备相对简单，已在谱仪系统中得到广泛应用。

球面弯晶谱仪通常采用Johann聚焦法[20-22]，其光源出光点和探测面都位于以球面半径为直径的Rowland圆上，在子午方向可以获得较好的光线聚焦效果和较高的光谱分辨率，但弧矢方向光线的发散会使总光通量急剧降低。通常实验室等离子体源强度有限，十分有必要优化光路结构，提高单能X射线源强。最早由FAENOV A Y提出的球面弯晶聚焦结构[23]，在子午方向利用晶体的Bragg衍射实现分光，在弧矢方向利用球面镜的几何性质实现光线聚焦，从而获得高亮度、大视场、高光谱和空间分辨率的单能装置；同时由于其光源和像面位置不再受限于Rowland圆上，光路设计更加灵活，适用于不同的空间条件。PIKUZ S A、ROSMEJ O N、RENNER O等在此基础上进一步优化结构，使其子午和弧矢方向的空间分辨率均得到提高，并在光谱诊断和重离子追迹实验中多次使用[24-27]。

本文开展了基于球面弯晶聚焦结构的高亮度桌面型单能X射线源的设计和实验。从Bragg衍射原理和球面镜聚焦公式出发，结合实际空间限制确定了光路参数；使用光线追迹软件模拟了Al靶$K\alpha_1$线经球面弯晶色散和聚焦后的光斑亮度和对应能谱展宽，与柱面弯晶衍射结果进行了比较；设计和装调了Al靶$K\alpha_1$线单能源的真空机械结构，开展了相应实验，并根据CCD成像结果讨论了获得的单能X射线亮度和能谱展宽。

1 单能X射线源光学设计

为了提高单能X射线源强，采用图1(a)所示的球面弯晶聚焦结构。该结构以球面弯晶为分光聚焦器件，通过优化物像距和角度关系，实现在子午方向色散，在弧矢方向聚焦，其中p是光源到弯晶的距离，q是弯晶到CCD探测面的距离，R是球面弯晶的曲率半径，也是相应的Rowland圆的直径，其在子午方向满足晶体的Bragg衍射条件，如图1(b)所示。一定能量范围的X射线经球面弯晶衍射在像面上线性色散，限束光阑位于探测面之前，选取光斑亮区并进一步提高目标能点单能性。在弧矢方向，物像距符合球面镜的几何聚焦关系为

$$\frac{1}{p}+\frac{1}{q}=\frac{2\sin\theta}{R} \tag{1}$$

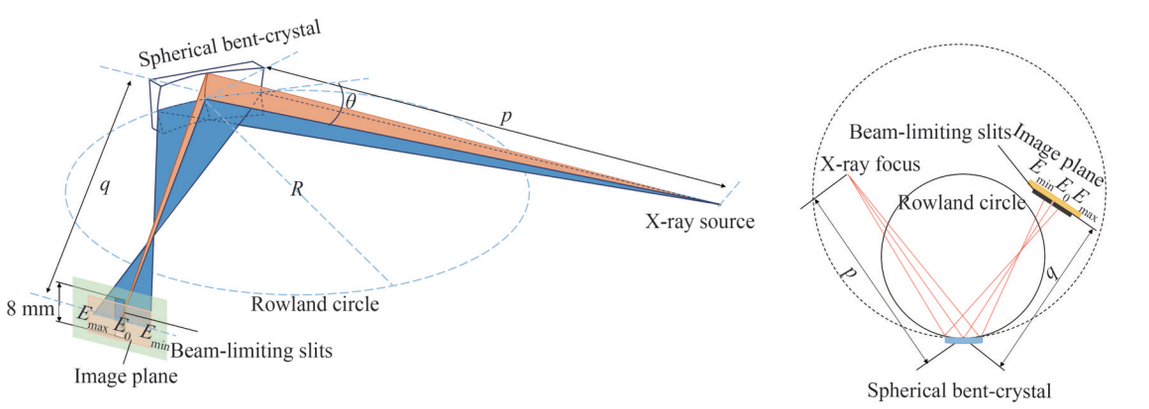

图1 球面弯晶聚焦结构示意图

Fig.1 Schematic diagram of the spherical bent-crystal focusing structure

基于球面弯晶聚焦结构，针对Al靶$K\alpha_1$线(1 486.70 eV)的单能需求确定光路具体参数。通常选择云母Mica(002)为Al靶$K\alpha_1$线单能晶体；为了提高色散程度，采用其二级衍射，并由Bragg条件确定相应的入射角，相应光路参数在表1中列出，此时弧矢方向由于光线聚焦可形成较亮的焦斑。

建立几何模型分析弧矢方向集光效率对谱线亮度的影响。以子午方向完全一致的球面弯晶和柱面弯

表1　针对Al靶$K\alpha_1$线的球面弯晶聚焦结构参数

Table 1　Parameters of the spherical bent-crystal focusing structure for Al $K\alpha_1$ line

Parameters	Values
Central Bragg angle/(°)	56.442 7
Range of Bragg angles/(°)	54.275 5～58.665 3
Range of dispersive energy/eV	1 450.48～1 526.07
Curvature radius of spherical bent-crystal/mm	250
Length/width of spherical bent-crystal/mm	50/8
Object distance/image distance/mm	337.51/270.01

晶作为分光器件，则谱线亮度的差异仅来自于弧矢方向不同的聚焦性能。定义η为球面与柱面弯晶所获谱线在弧矢方向单位长度的集光效率之比，其进一步等效为接收张角之比。图2(a)和(b)分别为球面弯晶和柱面弯晶在弧矢方向的等效透射光路示意图，其中s和l分别为物高和像高，p和q分别为物距和像距，M为垂轴放大率。计算得到η接近20，即球面弯晶的弧矢聚焦将谱线亮度提升了近20倍。

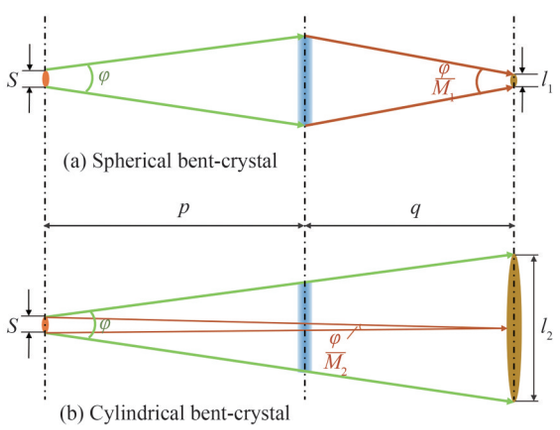

图2　弧矢方向等效光路示意图

Fig.2　Schematic diagram of the equivalent optical structure in the sagittal plane

2　光路性能模拟

通过光学仿真模拟球面弯晶聚焦结构得到的谱线亮度和展宽。使用基于Python语言的开源软件X-Ray Tracer (XRT)[28]，依据表1所示结构参数追迹等能量间隔的离散谱线，在像面处获得了均匀排布的光斑，其线性能量-空间关系为2.27 eV/mm。

同样的结构下追迹Al靶$K\alpha_1$线，设置其线宽为300 meV[29]。图3(a)是全视场条件下，Al靶$K\alpha_1$线经球面弯晶色散和聚焦得到的光斑，其中z轴指示子午(色散)方向，x轴指示弧矢(聚焦)方向；上方和右侧框图分别显示其在聚焦方向和色散方向的光强投影。图3(b)为能谱光强分布及其高斯拟合曲线，其半高宽约为0.259 mm，对应能谱展宽约为0.588 eV，能谱积分光子计数接近2×10^4。在像面前设置200 μm限束光阑，能谱展宽进一步缩小至0.454 eV，能谱积分光子计数约为1×10^4。

采用柱面弯晶作为色散器件，比较其与球面弯晶的聚焦效果。柱面弯晶在子午方向与球面弯晶具有相同的曲率半径且光路完全一致，其在弧矢方向等效为平面，没有聚焦效果。图4(a)中，全视场条件下Al靶$K\alpha_1$线的像斑呈带状分布，在z方向(色散方向)的宽度与图3(a)的结果大致相等，但在x轴方向(空间方向)上宽度显著增加。图4(b)的拟合结果显示二者能谱展宽基本一致，但其积分亮度相比于球面弯晶降低了一个数量级。采用不同的排布方式，使柱面弯晶的轴线方向与光路子午方向重合，此时其在弧矢方向和球面弯晶具有相同的曲率半径，而在子午方向等效为平晶。相比于球面弯晶，其谱线展宽增加了一倍，积分光子数降低了一半。

对比球面弯晶与不同排布方式的柱面弯晶所获谱线结果，证明了球面弯晶聚焦结构在保证能谱展宽的前提下，有效提高了谱线亮度。

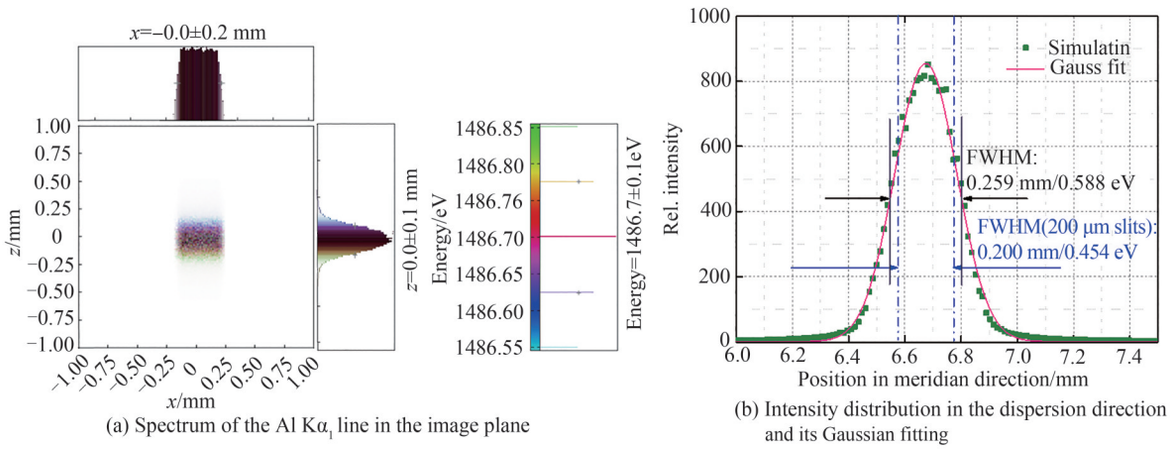

(a) Spectrum of the Al $K\alpha_1$ line in the image plane

(b) Intensity distribution in the dispersion direction and its Gaussian fitting

图 3 Al靶 $K\alpha_1$ 线经球面弯晶色散和聚焦的XRT追迹结果

Fig.3 XRT tracing results of Al $K\alpha_1$ line dispersed and focused by spherical bent-crystal

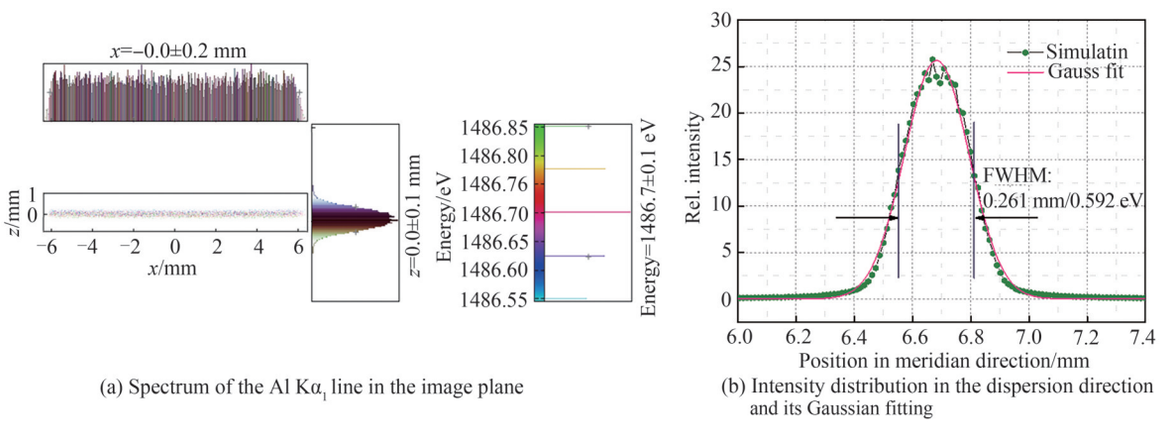

(a) Spectrum of the Al $K\alpha_1$ line in the image plane

(b) Intensity distribution in the dispersion direction and its Gaussian fitting

图 4 Al靶 $K\alpha_1$ 线经柱面弯晶衍射的XRT追迹结果

Fig.4 XRT tracing results of Al $K\alpha_1$ line diffracted by cylindrical bent-crystal

3 真空单能装置机械设计及实验分析

3.1 真空单能装置机械设计

由于空气对软X射线有吸收作用，因此需要设计一套真空装置用于实验。其主要结构包括：1)Al靶X射线管；2)真空腔体；3)弯晶组件；4)限束光阑；5)X射线CCD。基于球面弯晶聚焦结构的具体参数，设计了紧凑型的真空腔室，如图5所示。其中，X射线管采用Mcpherson公司Model642型Manson源，焦点直径约

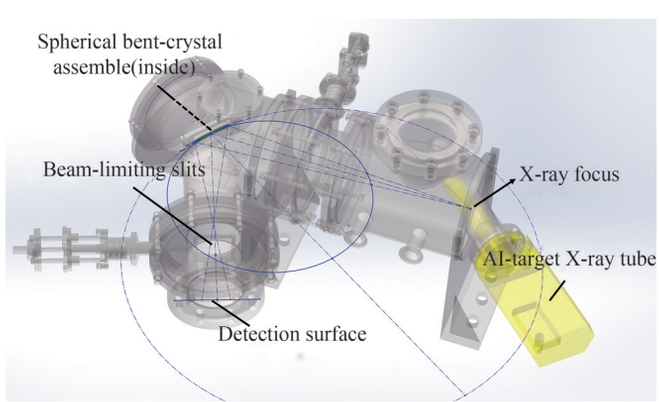

图 5 球面弯晶聚焦结构的真空机械设计

Fig.5 The vacuum mechanical design of the spherical bent-crystal focusing structure

1 mm；真空腔体材料为304不锈钢，通过法兰密封及分子泵抽气实现超高真空环境；云母弯晶由光敏胶粘合的方式获得，通过弯晶组件处的调节机构控制姿态；限束光阑用于选择光谱亮区并进一步提高单能性，在此装置中设计其子午方向宽度为200 μm，位置可调；X射线CCD采用Princeton Instruments公司的PIXIS-XO-1024B型号，面元尺寸为13.3 mm×13.3 mm，单像素尺寸为13 μm×13 μm，像面前放置5 μm厚度的铝箔以屏蔽可见光干扰，其在1.487 keV处透过率约为55%。大气环境下，使用半导体激光指示中心主光轴，完成系统装调。

3.2 实验及结果分析

X射线管工作电压和管流分别为7 kV和0.1 mA，即功率为7 W。光学器件依据表1所列结构参数排布，其几何关系由机械加工精度保证。图6(a)为X射线CCD曝光10 min得到的全视场Al靶$K\alpha_1$线能谱，其水平和竖直方向分别为色散和聚焦方向。图6(b)用高斯线型拟合了色散方向的光强分布曲线，单像素的探测器计数峰值大于1.2×10^4，能谱计数大于2×10^5；其半高宽为0.261 mm，根据线色散关系计算其能谱展宽为0.592 eV，与模拟结果基本一致。

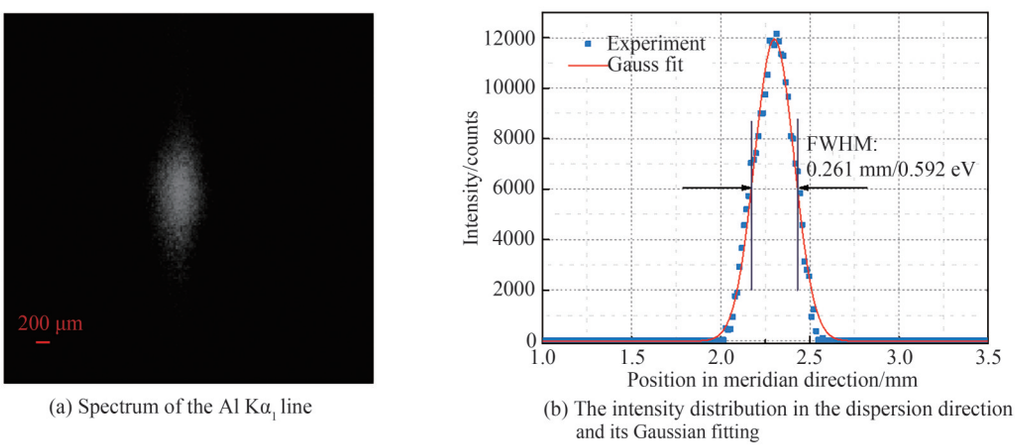

(a) Spectrum of the Al $K\alpha_1$ line

(b) The intensity distribution in the dispersion direction and its Gaussian fitting

图6 无限束光阑的实验结果

Fig.6 Experimental results without a beam-limiting slit

为进一步优化能谱展宽，引入200 μm限束光阑，再次用X射线CCD曝光10 min，得到如图7(a)所示光斑，单像素计数峰值大于3 000，能谱计数约为2×10^4；图7(b)中的拟合结果显示光斑半高宽约为0.217 mm，对应能谱展宽约为0.493 eV。由于光阑与CCD像面之间约有50 mm的实际距离，导致展宽略大于模拟结果。

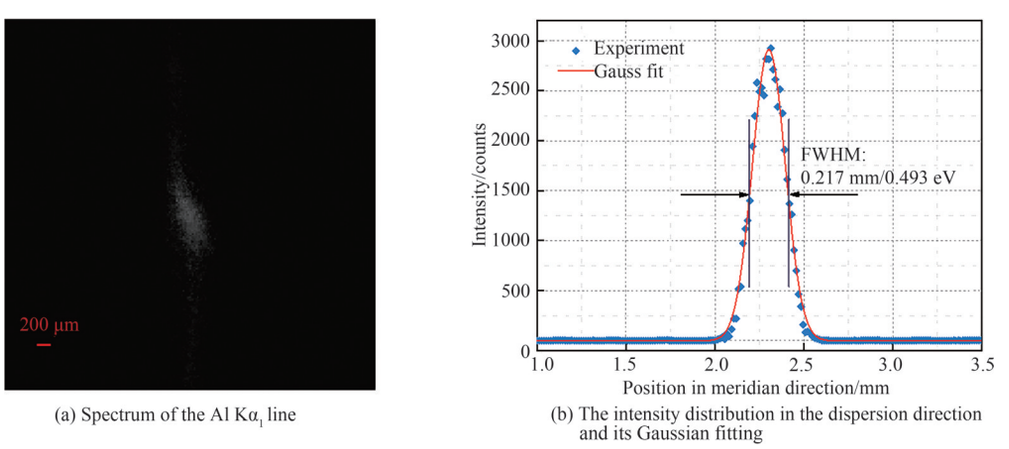

(a) Spectrum of the Al $K\alpha_1$ line

(b) The intensity distribution in the dispersion direction and its Gaussian fitting

图7 引入200 μm限束光阑的实验结果

Fig.7 Experimental results with a 200 μm beam-limiting slit

4 结论

本文提出了一种基于球面弯晶聚焦结构的高亮度桌面型X射线单能方法，设计了在子午和弧矢方向分别实现光线色散和聚焦的光学结构，模拟了像面处谱线的亮度和相应的能谱展宽，据此搭建了一套单能X射线源。理论计算和光学仿真的结果均验证了球面弯晶聚焦结构对能谱亮度的有效提升。实验结果表明，Al靶$K\alpha_1$线经该装置聚焦后，10 min曝光条件下，能谱的CCD计数大于2×10^5，谱线展宽约为0.592 eV；引入200 μm限束光阑，将能谱展宽减小至0.493 eV，能谱计数约为2×10^4，证明了该装置在聚焦特性上的显著优势。在未来，通过使用微焦点X射线管、更换晶格更小的弯晶或缩小光阑宽度等方式可以进一步提升源强条件和单能性，为精确测量光学器件及系统的光谱特性提供了一种新的技术途径。

参考文献

[1] SINARS D B, GREGORIAN L, HAMMER D A, et al. Plasma imaging and spectroscopy diagnostics developed on 100-500-kA pulsed power devices[J]. Proceedings of the IEEE, 2004, 92(7): 1110-1121.

[2] MCDONALD S A, BURNETT T L, DONOGHUE J, et al. Tracking polycrystal evolution non-destructively in 3D by laboratory X-ray diffraction contrast tomography[J]. Materials Characterization, 2021, 172: 110814.

[3] PATTERSON B M, CAMPBELL J, HAVRILLA G J. Integrating 3D images using laboratory-based micro X-ray computed tomography and confocal X-ray fluorescence techniques[J]. X-Ray Spectrometry, 2010, 39(3): 184-190.

[4] O'DELL S L, ATTINÀP, BALDINI L, et al. The Imaging X-Ray Polarimetry Explorer (IXPE): technical overview II [C]. UV, X-Ray, and Gamma-Ray Space Instrumentation for Astronomy XXI, International Society for Optics and Photonics, 2019.

[5] SOFFITTA P, BARCONS X, BELLAZZINI R, et al. XIPE: The X-ray imaging polarimetry explorer[J]. Experimental Astronomy, 2013, 36(3): 523-567.

[6] SOKOLOV A, HUANG Q, SENF F, et al. Optimized highly efficient multilayer-coated blazed gratings for the tender X-ray region[J]. Optics Express, 2019, 27(12): 16833.

[7] ECKART M E, ADAMS J S, BOYCE K R, et al. Ground calibration of the Astro-H (Hitomi) soft X-ray spectrometer [J]. Journal of Astronomical Telescopes, Instruments, and Systems, 2018, 4(2): 021406.

[8] ZHOU Hongjun. Higher order harmonics suppression research and key components developing of spectral radiation standard and metrology beamline[D]. Hefei: University of Science and Technology of China, 2006
周洪军. 光谱辐射标准和计量线站高次谐波抑制研究和关键部件研制[D]. 合肥：中国科学技术大学, 2006.

[9] Thermofisher. Sequential X-ray fluorescence spectrometer XR-BR41270 manual[E/OL]. https://assets.thermofisher.com/TFS-Assets/MSD/brochures/XR-BR41270-arl-performx-spectrometer.pdf.

[10] BRUKER. X-ray diffraction D8 DISCOVER manual[E/OL]. https://www.bruker.com/en/products-and-solutions/diffractometers-and-x-ray-microscopes/x-ray-diffractometers/d8-discover-family/d8-discover.html.

[11] LOUIS E, YAKSHIN A E, TSARFATI T, et al. Nanometer interface and materials control for multilayer EUV-optical applications[J]. Progress in Surface Science, 2011, 86(11-12): 255-294.

[12] RACK A, WEITKAMP T, RIOTTE M, et al. Comparative study of multilayers used in monochromators for synchrotron-based coherent hard X-ray imaging[J]. Journal of Synchrotron Radiation, 2010, 17(4): 496-510.

[13] SCHICK D, BOJAHR A, HERZOG M, et al. Normalization schemes for ultrafast X-ray diffraction using a table-top laser-driven plasma source[J]. Review of Scientific Instruments, 2012, 83(2): 025104.

[14] PARK J, BROWN G V, SCHNEIDER M B, et al. Calibration of a flat field soft X-ray grating spectrometer for laser produced plasmas[J]. Review of Scientific Instruments, 2010, 81(10): 10E303.

[15] HEILMANN R K, BRUCCOLERI A R, SCHATTENBURG M L. High-efficiency blazed transmission gratings for high-resolution soft X-ray spectroscopy[C]. Optics for EUV, X-Ray, and Gamma-Ray Astronomy VII, SPIE, 2015, 9603: 296-307.

[16] SCHOLLMEIER M S, LOISEL G P. Systematic search for spherical crystal X-ray microscopes matching 1-25 keV spectral line sources[J]. Review of Scientific Instruments, 2016, 87(12): 123511.

[17] HU Ruijie. High-performance upgrade of X-ray crystal spectrometer and experimental study of ICRF flow drive on EAST [D]. Hefei: University of Science and Technology of China, 2019.
胡睿佶. EAST 弯晶谱仪高性能升级及离子回旋波驱动旋转的实验研究[D]. 合肥：中国科学技术大学, 2019.

[18] PHILLIPS, JH K, KENT B J, et al. Solar flare X-ray spectra from the solar maximum mission flat crystal spectrometer [J]. Astrophysical Journal, 1982, 256(2): 774-787.

[19] MISSALLA T, USCHMANN I, FÖRSTER E, et al. Monochromatic focusing of subpicosecond X-ray pulses in the keV range[J]. Review of Scientific Instruments, 1999, 70(2): 1288-1299.

[20] BITTER M, HILL K, ROQUEMORE L, et al. Results from the national spherical torus experiment X-ray crystal

spectrometer[J]. Review of Scientific Instruments, 2003, 74(3): 1977-1981.
[21] LEE S G, YOO J W, KIM Y S, et al. Experimental results from an X-ray imaging crystal spectrometer utilizing multi-wire proportional counter for KSTAR[J]. Review of Scientific Instruments, 2016, 87(11): 11E314.
[22] YAN W, CHEN Z Y, JIN W, et al. Measurement of the electron and ion temperature by the X-ray imaging crystal spectrometer on joint Texas experimental tokamak[J]. Review of Scientific Instruments, 2016,87(11): 11E318.
[23] FAENOV A Y, PIKUZ S A, Erko A I, et al. High-performance X-ray spectroscopic devices for plasma microsources investigations[J]. Physica Scripta, 1994, 50(4): 333.
[24] PIKUZ S A, EFREMOV V P, ROSMEJ O, et al. Investigations of heavy-ion tracks′ energy deposition inside solid media by methods of X-ray spectroscopy[J]. Journal of Physics A: Mathematical and General, 2006, 39(17): 4765.
[25] ROSMEJ O N, WIESER J, GEISSEL M, et al. X-ray spectromicroscopy of fast heavy ions and target radiation[J]. Nuclear Instruments and Methods in Physics Research Section A: Accelerators, Spectrometers, Detectors and Associated Equipment, 2002, 495(1): 29-39.
[26] ROSMEJ O N, PIKUZ JR S A, WIESER J, et al. Investigation of the projectile ion velocity inside the interaction media by the X-ray spectromicroscopy method[J]. Review of Scientific Instruments, 2003, 74(12): 5039-5045.
[27] RENNER O, SAUVAN P, DALIMIER E, et al. X-ray spectroscopy of hot dense plasmas: experimental limits, line shifts & field effects[C]. AIP Conference Proceedings, American Institute of Physics, 2008, 1058(1): 341-348.
[28] KLEMENTIEV K, CHERNIKOV R. Powerful scriptable ray tracing package xrt[C]. Advances in Computational Methods for X-Ray Optics III, SPIE, 2014, 9209: 60-75.
[29] FARACI G, PENNISI A R, GOZZO F, et al. Cs bonding at the Cs/GaAs (110) interface[J]. Physical Review B, 1996, 53(7): 3987.

Design and Experimental Study of a Desktop Monochromatic X-ray Source Based on Spherical Bent-crystal Focusing Structure

YU Yue[1,2], SI Haoxuan[1,2], YANG Zuhua[3], YI Shengzhen[1,2], WANG Zhanshan[1,2]
(1 *Institute of Precision Optical Engineering, School of Physics Science and Engineering, Tongji University, Shanghai* 200092, *China*)
(2 *MOE Key Laboratory of Advanced Micro-Structured Materials, Tongji University, Shanghai* 200092, *China*)
(3 *Laser Fusion Research Centre, China Academy of Engineering Physics, Mianyang* 621900, *China*)

Abstract: X-ray optics and systems have been widely used for applications such as plasma diagnostics, X-ray spectroscopy, astronomical observation and material analysis. The spectral characteristics of the optics and systems need to be accurately measured, for which a high-brightness monochromatic X-ray source is indispensable. Synchrotron radiation facilities provide the most reliable metrology, but their measurement timeliness is limited because of the allocated user beam time and long distances to reach the facilities. Commercial X-ray measurement equipment, such as X-ray fluorescence spectrometers, X-ray reflectometers and diffractometers, are only capable of measurements of small-size optics at a few fixed energy points. Desktop monochromatic X-ray sources that combine X-ray tubes with dispersive optics have provided a laboratory-based approach to calibrating X-ray optics, where the dispersive optics usually refers to multilayers, gratings and crystals. Multilayers are distinguished by their high luminous flux and wide working energy band, but their spectral resolution is relatively low; X-ray gratings allow for much higher spectral resolution, but the fabrication processes are quite difficult for extremely dense grooves for X-ray diffraction. Crystals have a naturally unique dispersion capability in the X-ray band that can substantially improve the spectral resolution. Common-used planar and cylindrical crystals have limited effects to enhance the system throughput because of relatively weak focusing capability in one or both dimensions; complex aspheric bent-crystals, such as toroidal, parabolic and hyperbolic crystals, can reduce aberrations and focus in both meridional and sagittal directions so that system throughput and spectral resolution can be significantly improved. However, aspheric bent-crystals are difficult to fabricate and have many limitations for application; and the aberration would deteriorate abruptly if the incident angle deviates from the designed value. Spherically bent-crystals enable two-dimensional focusing and are relatively easy to be fabricated; therefore, they have been widely used in X-ray spectrometers. Conventional spherical

bend-crystal spectrometers adopt the Johann scheme, where the light source and the image plane are located on a Rowland circle with a diameter equaling to the radius of the concave bend-crystal. By applying Johann scheme, better focusing and higher spectral resolution are obtained in the meridional direction, but the brightness of the spectral lines acquired in the image plane is largely decreased due to light divergence in the sagittal direction. Therefore, it is necessary to optimize the optical structure to improve the intensity of dispersed monochromatic X-ray. In this paper, a desktop method for obtaining high-brightness monochromatic X-ray is proposed based on a spherical bent-crystal focusing structure. It achieves monochromaticity in the meridional direction using crystal dispersion, and obtains high brightness in the sagittal direction simultaneously based on spherical-mirror focusing. A geometric model is developed to theoretically compare the efficiency of collecting light of the spherical and cylindrical bent-crystals; also, the dispersion and focusing performance of different optical layouts with spherical and cylindrical bent-crystals are simulated and evaluated. Both theoretical and simulation results show that the spherical bent-crystal focusing structure has an excellent performance in terms of focusing characteristics, with the brightness of the spectral line obviously increased, compared with the cylindrical bent-crystal. In view of the monochromatizing requirements of the Al $K\alpha_1$ line, a device based on low-power Al-target X-ray tube is designed and adjusted, and its performance was tested by spectroscopic experiments. Measurement results show that with the X-ray tube working at 7 W power and CCD exposure for 10 minutes, the count of the full-field spectrum of the Al $K\alpha_1$ line is greater than 2×10^5 with a spectral broadening of about 0.592 eV; when introducing a 200 μm beam-limiting slit, the spectral broadening is further reduced to 0.493 eV and the CCD count is about 2×10^4. The results have verified that the device can effectively obtain the high-brightness Al $K\alpha_1$ line, and also provides a new technical approach for accurately measuring the spectral characteristics of X-ray optics and systems.

Key words: Spherical bent-crystal focusing structure; High intensity; High monochromaticity; Desktop; X-ray source

OCIS Codes: 340.7480; 300.6560; 300.6320; 120.4570

Foundation item: National Key Research and Development Program of China (Nos. 2022YFA1603500, 2019YFE03080200), National Natural Science Foundation of China (Nos. 11875202, 12105268)